

Lattice study of the Kink soliton and the zero-mode problem for ϕ^4 in two dimensions

A. Ardekani and A. G. Williams

Department of Physics and Mathematical Physics
Special Research Center for the Subatomic Structure of Matter,
University of Adelaide, SA 5005, Australia

Abstract

We study the $\lambda\phi_{1+1}^4$ kink soliton and the zero-mode contribution to the Kink soliton mass in regions beyond the semiclassical regime. The calculations are done in the non-trivial scaling region and where appropriate the results are compared with the continuum, semiclassical values. We show, as a function of parameter space, where the zero-mode contributions become significant.

* aardekan@physics.adelaide.edu.au

† awilliam@physics.adelaide.edu.au

Solitons are non-dispersive localised packets of energy moving uniformly, and resembling extended particles. The elementary particles in nature are also localised packets of energy, being described by some quantum field theory. Because of these features, the soliton might appear as the ideal mathematical structure for the description of a particle. When it was realised that many nonlinear field theories used to describe elementary particles, also had soliton solutions and that these solutions might correspond to particle type excitations, the development of methods for soliton quantisation became important. The quantisation of solitons is usually done by performing an expansion in powers of \hbar (loop expansion) such that the classical soliton solution appears as the term of leading order in the expansion and terms of higher order represent the quantum effects. In the mid 1970's there appeared a number of works [1–4] which developed the semiclassical expansion in the quantum field theory. In this period, there were schemes being constructed to quantise these solitons. The correspondence between classical soliton solutions and extended-particle states of the quantised theory were established [1,3,5]. Collective coordinate methods were used to deal with the so-called “zero-mode problem” [6–9]. This problem is a manifestation of the translational invariance of the theory, broken by the introduction of the soliton. Field oscillations around this classical solution contain zero frequency modes, describing displacements of the soliton.

Here we study the mass of the simplest topological soliton, that is the $\lambda\phi_{1+1}^4$ kink, using lattice Monte Carlo techniques. The dynamics of this model are governed by a Euclidean Lagrangian density

$$\mathcal{L} = \frac{1}{2}(\partial_\mu\phi)^2 - \frac{\mu^2}{2}\phi^2 + \frac{\lambda}{4}\phi^4, \quad (1)$$

where μ is a bare parameter and λ is the bare coupling constant. For a free scalar field theory $\lambda \rightarrow 0$ and $-\mu^2 \rightarrow 0$, where m would then be the mass ϕ . There are two types of static solutions, both being static solutions, to the equation of motion; the trivial solutions

$$\phi_0 = \pm \frac{\mu}{\sqrt{\lambda}} \equiv f, \quad (2)$$

and the topological solutions

$$\phi_{k,ak} = \pm \frac{\mu}{\sqrt{\lambda}} \tanh\left[\frac{\mu}{\sqrt{2}}x\right], \quad (3)$$

where k and ak label the topological solutions with the kink and antikink correspond to the positive and negative sign, respectively. The semiclassical regime corresponds to large f .

The kink provides an example of a particle with an internal structure, distributed over a finite volume rather than concentrated at one point. It possesses a nonzero, conserved quantity called the topological charge Q which is defined as

$$Q = [\phi(x)|_\infty - \phi(x)|_{-\infty}]$$

and which leads to stability of the kink solution. The classical kink mass M_{cl} , is defined the energy of the static soliton and is given by

$$M_{\text{cl}} = \frac{2\sqrt{2}\mu^3}{3\lambda}. \quad (4)$$

The vacuum and kink solutions can be quantised by path integral quantisation or by construction of a tower of approximate harmonic oscillator states around the classical solution $\bar{\phi}$, where $\bar{\phi} = \bar{\phi}_0, \phi_k$ or ϕ_{ak} . In a finite box with the length L the soliton mass with a one loop quantum correction becomes [10]:

$$M_{\text{sol}} = E_{\text{kink}} - E_{\text{vac}} = M_{\text{cl}} + \sum_n \frac{1}{2}\omega_n^2 - \sum_n \frac{1}{2}\xi_n^2 + \mathcal{O}(\hat{\lambda}), \quad (5)$$

where ω_n and ξ_n are the eigenvalues of the following equation

$$\left[-\frac{\partial^2}{\partial x^2} + (3\lambda\phi^2 - 2\mu^2)_{\bar{\phi}} \right] \eta_i(x) = \Theta_i^2 \eta_i, \quad (6)$$

with $\bar{\phi} = \phi_0$ and $\bar{\phi} = \phi_k$ or ϕ_{ak} for ω_n and ξ_n respectively. An important point to note is that, due to translational invariance, one of the ω 's is zero, i.e, $\omega_0 = 0$.

As L is set to infinity then the sums are replaced by integrals and one ends up with a logarithmically divergent integral and renormalisation is required to render the kink mass finite. Then one arrives at the mass of the continuum kink with one loop corrections [3]:

$$M_{\text{sol}} = \frac{2\sqrt{(2)}}{3\lambda}\mu^3 + \mu\left(\frac{1}{6}\sqrt{\frac{3}{2}} - \frac{3}{\pi\sqrt{2}}\right) + \mathcal{O}(\lambda). \quad (7)$$

The zero eigenvalue $\omega = 0$ is referred to as the zero-mode and has well known physical consequences. These modes always exist when one quantises a theory with a translational invariant Lagrangian about a solution that is not translational invariant. The physical consequence of the existence of the zero-mode is the center of mass motion of the kink. In Eq. (7) the zero-mode contribution to the kink mass is omitted. That effectively means that the mass of the quantum kink particle is assumed to be the same as the kink energy. The semiclassical treatment of these zero-modes is done in variety of ways [1,11–13], however, we will not discuss these further here, since it is not necessary for our purpose. It is also important to mention that the semiclassical quantisation of the discrete lattice version of the lagrangian density given by Eq. (1) in a finite size box is also complicated by the zero-mode problem.

Kink on the lattice

The $\lambda\phi^4$ action on a 2-d lattice can be written as:

$$S = - \sum_{n,\mu} \phi_n \phi_{n+\mu} + \sum_n \left(2 - \frac{\hat{\mu}^2}{2} \right) \phi_n^2 + \frac{\hat{\lambda}}{4} \phi_n^4 \quad (8)$$

where we have defined the dimensionless quantities $\hat{\mu} \equiv \mu a$ and $\hat{\lambda} \equiv \lambda a^2$ with a being the lattice spacing. In addition $n \equiv (n_1, n_2)$ is a 2-dimensional vector labeling the lattice sites and μ is a unit vector in the temporal or spatial direction (not to be confused with our parameter $\mu^2 \equiv -\widehat{m}^2$). We also have denoted the field on the neighboring site of n in the direction of μ by $\phi_{n,\mu}$.

This model exhibits two phases. In some regions of the phase space, the symmetric regions, $\langle \phi \rangle = 0$ whereas in other regions spontaneous symmetry breaking occurs and $\langle \phi \rangle \neq 0$. Classically, for positive values of $\widehat{m}^2 \equiv -\hat{\mu}^2$ one always has $\langle \phi \rangle = 0$ and for negative \widehat{m}^2 (i.e., positive $\hat{\mu}^2$), where spontaneous symmetry breaking occurs, $\langle \phi \rangle \neq 0$. In this regime the second order critical line which separates two phases is the line corresponding to the line $\widehat{m}^2 = 0$. Beyond the classical limit the phase space structure changes. There still the two phases and there is still a second order phase critical line separating these phases, however, the position of the critical line changes and in general due to quantum fluctuations occurs at a finite negative \widehat{m}^2 .

In order to determine the critical line, we choose several values of $\widehat{m}^2 < 0$ located in the broken symmetry sector where $\langle \phi \rangle \neq 0$. For each value of \widehat{m}^2 , $\hat{\lambda}$ can be increased until $\langle \phi \rangle = 0$ and, thus, the critical parameters, $(\widehat{m}_c^2, \hat{\lambda}_c)$, can be found. Of course there is no second order phase transition on a finite lattice, however, by a second order phase transition here we mean that the correlation length is much larger than the lattice dimensions. The critical line is shown in Fig. 1. We have also shown in this figure the one loop prediction for the critical line using the light-front formulation [15].

The authors of Ref. [16] proposed two methods of calculating the kink mass on the lattice. Here we use one of these methods which uses a local parameter and is much less susceptible to finite size effects. In this method one imposes an anti-periodic spatial boundary condition, giving rise to a topological excitation with non-zero topological charge. Since the kink has the lowest energy in the topological sector this topological excitation corresponds to the kink. It is shown that for a fixed \widehat{m} , one has [16]:

$$M_{\text{sol}}(\hat{\beta}) = \int_{\beta_c}^{\hat{\beta}} d\beta' \Omega(\beta') \equiv \frac{1}{T} \int_{\beta_c}^{\hat{\beta}} d\beta' \frac{1}{\beta'} [\langle S_a \rangle - \langle S_p \rangle], \quad (9)$$

where M_{sol} is the soliton mass, $\hat{\beta} = 1/\hat{\lambda}$, $\hat{\beta}_c$ is the inverse of the dimensionless critical bare coupling $\hat{\lambda}_c$, T is the length of the lattice in the temporal direction, $\langle S_p \rangle$ and $\langle S_a \rangle$ are the mean action of the system with a periodic and anti-periodic spatial boundary condition, respectively.

As we mentioned earlier in the semiclassical quantisation one encounters the zero-mode problem with its physical consequences being the center of mass motion of the kink. An interesting question is whether this problem persists beyond the semiclassical regime. To answer whether the zero-mode problem persists beyond the semiclassical regime, one can examine one of the consequences of the existence of a zero-mode, that is, the kink displacements. On a lattice with anti-periodic boundary condition in the special direction, we set $\widehat{m}^2 \equiv -\mu^2 = -1$

and $\hat{\lambda} = 4$ giving $f = 0.5$, which corresponds to a region beyond the semiclassical regime. Then for an arbitrary time slice we calculated $\langle \phi_n \rangle$ for each site for a number of configurations and an average over these configurations was calculated. We have shown the results in Fig. 2. As this figure suggests, the movement of the kink due to the translational mode still persists even beyond the semiclassical regime. We repeated the same procedure for different time slices and different number of sampled configurations and lot of the results showed the same behaviour.

In order to treat the problem, we imposed an additional constraint, that is $\phi(M) = 0$ with $M = (x_0, N/2)$ for all times x_0 , fixing the center of the kink to the center of the lattice. For the same time slices as in the previous case and for a number of constrained configurations, the value of $\langle \phi_n \rangle$ for each site along with the classical configuration are included in Fig. 2. The constrained configuration resembles the kink solution with its center located at the center of the lattice.

Both in numerical MC studies and the analytical calculations it is important to find the renormalisation group trajectories (RGT). Along these curves and close to an infrared (IR) fixed point the physics described by the lattice regularised quantum field is constant and only the value of the cut-off (lattice spacing) is changing. This region is called the scaling region. The $\lambda\phi^4$ theory in two dimension is an interacting theory. That is, in addition to having a Gaussian fixed point at $\widehat{m}^2 = \hat{\lambda} = 0$ where the renormalised coupling $\hat{\lambda}_r$ vanishes, it has other infrared fixed points at which $\hat{\lambda}_r$ is non-zero. The best candidates for these fixed points are along the critical line where a second order phase transition occurs. In this model the only non trivial critical region is along the transition line shown in Fig. 1. In the vicinity of the fixed point the vertex functions strongly scale [17] and one expects that close to the critical line, there should be segments of phase space where the ratios of dimensionless vertex functions remain almost constant, giving the scaling region.

In our calculations it is important to find the scaling region corresponding to a non-trivial IR fixed point. That is, one should try to find trajectories away from the Gaussian fixed point. On trivial fixed point trajectories, even though the spontaneous symmetry breaking can still occur and a kink solution can exist, the vacuum is governed by a free field. We used $R(\widehat{m}_r, \hat{\lambda}_r) \equiv \widehat{m}_r^2 / \hat{\lambda}_r$ as a dimensionless parameter for probing the scaling region. This parameter R , can be calculated accurately using the effective potential method [18]. The scaling region corresponds to regions where R is approximately constant. Our entire calculations are performed within the scaling region so that they can be legitimately compared with the continuum-semiclassical predictions for the soliton mass, given by Eq. (7).

For a fixed value of $\widehat{m}^2 = -1$ we found a range of values of $\hat{\lambda}$ in the broken symmetry sector, that is $0.2 < \hat{\lambda} < 0.8$, for which the values of $R(\widehat{m}_r, \hat{\lambda}_r)$ were approximately constant, determining a segment of the scaling region corresponding to $\widehat{m}^2 = -1$. Then for some values of $\hat{\lambda}$ within this region we calculated $\Delta S = \langle S_a \rangle - \langle S_p \rangle$. In calculations of $\langle S_a \rangle$ we constrained

the center of the kink to the center of the lattice. We have plotted $\Delta S/T$ versus $\hat{\beta}$ along with its classical value in Fig. 3. Having known $\Delta S/T$, Eq. (9) can be used to calculate the soliton mass. We also calculated the soliton mass with and without imposing a constraint on the center of the kink. The comparison of these results with each other and with the classical and semiclassical values is shown in Fig. 4. As is evident, in this case the zero-mode contribution is within statistical uncertainties. The statistical uncertainties, as one expects, increase as one approaches the critical line which makes the detection of the zero-mode contribution to soliton mass difficult. Also, it is interesting to note that the Monte Carlo results for the soliton mass are less than the classical mass but larger than one loop semiclassical predictions.

Next, for $\widehat{m}^2 = -2.2$, we repeated the same procedure and calculated the soliton mass for a number of bare couplings within the scaling region. The calculations were done with and without a constraint on the center of the kink and the results and their comparison with the classical and semiclassical predictions are shown in Fig. 5. Our results are consistent with Ref. [16]. There are two important observations. First, unlike the previous case the MC calculated soliton masses are lower than the semiclassical values which is due to the higher order corrections. The other important point is that, close to the critical line it appears to be positive that there is a positive contribution to the soliton mass due to the zero-mode.

Finally, for $\widehat{m}^2 = -4$ we calculated the soliton mass, with and without a constraint on the configurations. The results are shown in Fig. 6 and again the zero-mode contribution to the soliton mass appears to be positive.

All our calculations were done on a 48×48 lattice. As one approaches the critical line the correlation length increases and the finite size effects become more significant. However, since the Monte Carlo calculation of masses are based on a local parameter $\Omega(\beta)$ the finite size effects are smaller than one might, in general, expect [19]. In our calculations we kept the correlation length below a half of the lattice length.

In conclusion we would like to mention that in addition to a straightforward elimination of the zero-mode, the imposition of a constraint on the center of the kink resulted also in more stable configurations and a reduction of the statistical uncertainties on $\langle S_a \rangle$ and consequently on M_{sol} . These instabilities are more significant close to the critical line where the field fluctuations are larger. In general we found that the statistical uncertainties on $\langle S_a \rangle$ were much larger than $\langle S_p \rangle$.

REFERENCES

- [1] R. Dashen, B. Hasslacher, A. Neveu, Phys. Rev. D **10**, 4114, (1974).
- [2] R. Friedberg, T.D. Lee, Phys. Rev. D **15**, 1694, (1997).
- [3] R. Dashen, B. Hasslacher, A. Neveu, Phys. Rev. D **10**, 4130, (1974).
- [4] R. Dashen, B. Hasslacher, A. Neveu, Phys. Rev. D **10**, 4138, (1974).
- [5] D.K. Campbell and Y.T. Liao, Phys. Rev. D **14**, 2093, (1976).
- [6] J.L. Gervais B. Sakita, Phys. Rev. D **12**, 2943, (1975).
- [7] J.L. Gervais B. Sakita, Phys. Rept. **23** 281-293, (1976).
- [8] L. D. Faddeev and V. E. Korepin Phys. Lett. B **63**, 435, (1976).
- [9] R. Rajaraman and E.J. Weinberg, Phys. Rev. D **11**, 2950, (1975).
- [10] R. Rajaraman, 'Solitons and Instantons', North Holland Physics Publishing, (1982).
- [11] J. Goldstone and R. Jakiw, Phys. Rev. D **11**, 1486, (1975).
- [12] A.M. Polyakov, JETP Lett. **20** 194, (1974).
- [13] N.H. Christ, T.D. Lee, Nucl. Phys. B **21**, 1606, (1975).
- [14] L.P. Kadanoff and H. Ceva, Phys. Rev. B **3**, 3918, (1971).
- [15] C. Bender, S. Pinsky and B.V. Sande, Phys.Rev. **D48**, 816, 1993.
- [16] J.C. Ciria and A. Tarancon, Phys. Rev. D **49**, 1020, (1994). Even though these results are consistent, our results indicate that the Monte Carlo values lie below the semiclassical predictions whereas the results in Ref. [16] show an opposite relation. (The discrepancy is due to an inadvertent error in the presentation of the semiclassical results.)
- [17] J. Zinn-Justin. Quantum field theory and critical phenomena. Oxford, UK: Clarendon (1993).
- [18] A. Ardekani and A. G. Williams Phys.Rev. **E57**, 6140, (1998).
- [19] J. Groeneveld, J. Jurkiewicz, C.P. Korthals Atles, Physica Scripta, **23**, 1022, (1981).

FIGURES

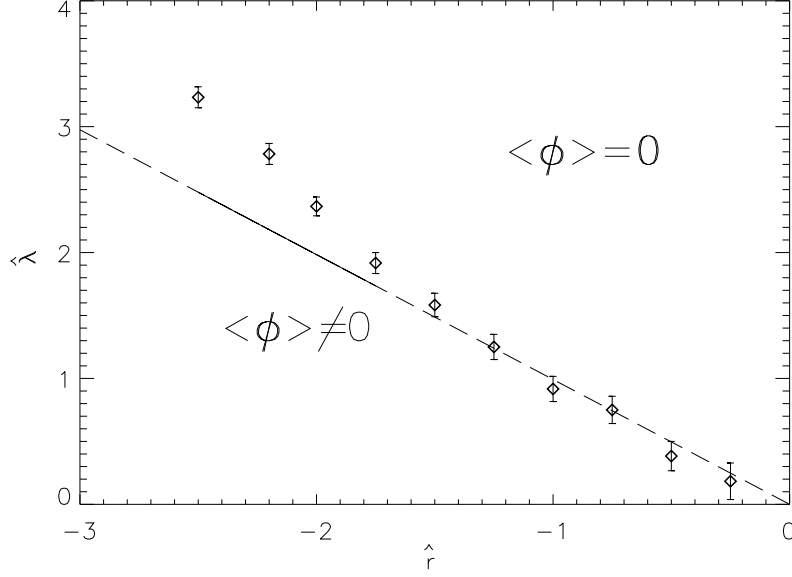


FIG. 1. The plot of the transition line between the broken sector and unbroken sector using Monte Carlo methods (diamond) and the light-front perturbative predictions (dashed line). We used the symbol $\hat{r} \equiv \hat{m}^2$ in the above figure.

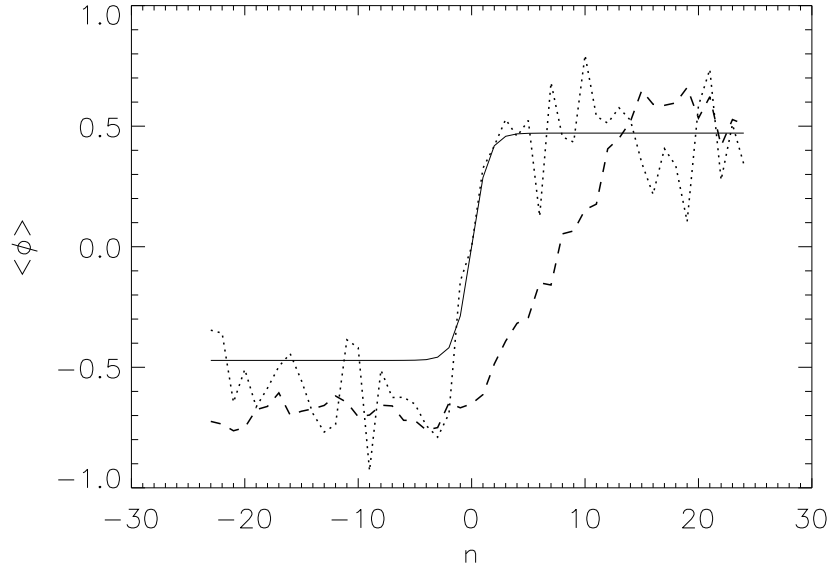


FIG. 2. The comparative plot of averages of fields on a time slice with $f = 0.5$ and $\hat{m}^2 = -1$ for a unconstrained lattice (dashed line) and constrained lattice (dotted line). The constraint fixes the center of the kink to the center of the lattice for all time slices. The solid line is the classical solution.

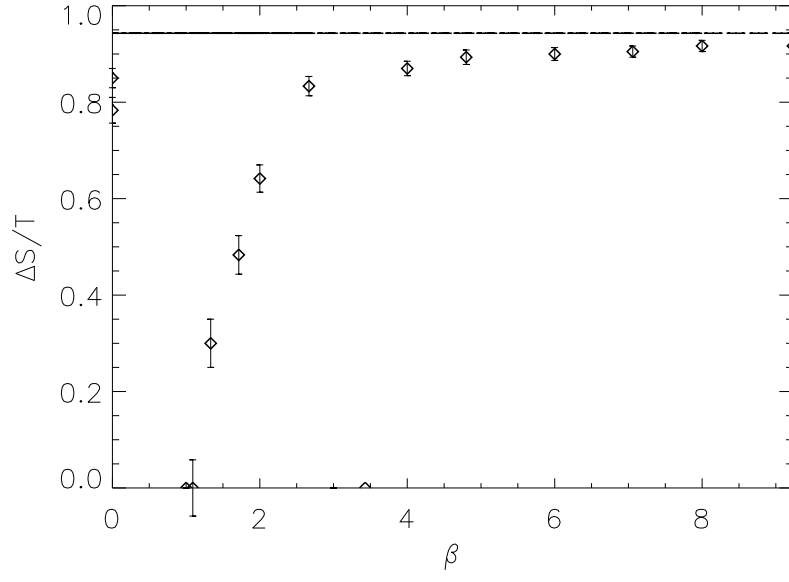


FIG. 3. The plot of $\Delta S/T$ versus $\hat{\beta} = 1/\hat{\lambda}$ with $\hat{m}^2 = -1.0$. The straight horizontal line is the classical value for $\Delta S/T$

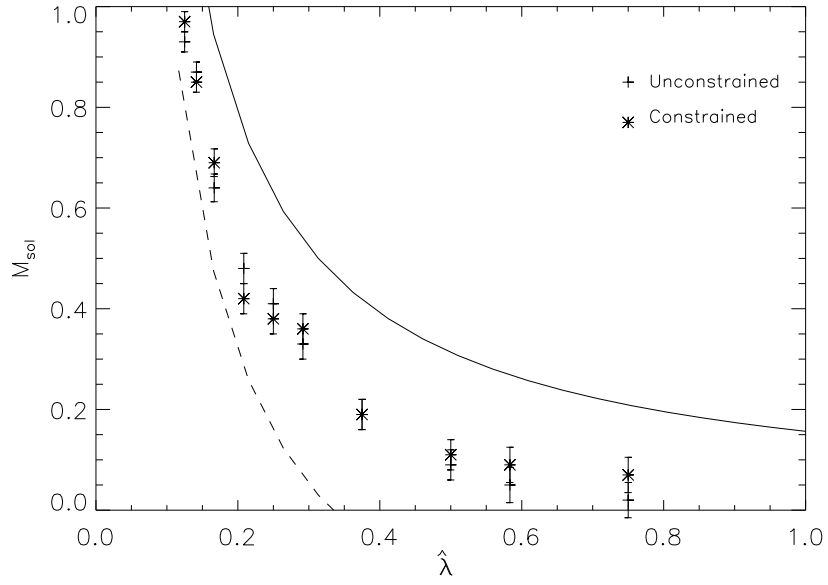


FIG. 4. Plot of soliton mass versus β with $\hat{m}^2 = -1$. The Monte Carlo results are compared with the classical (solid line) and semiclassical results (dashed line).

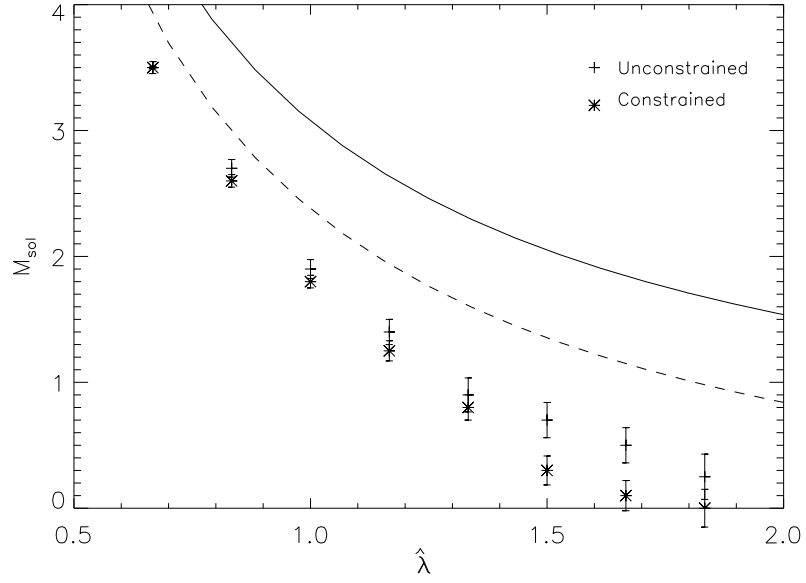


FIG. 5. Plot of soliton mass versus β with $\hat{m}^2 = -2.2$. The Monte Carlo results are compared with the classical (solid line) and semiclassical results (dashed line).

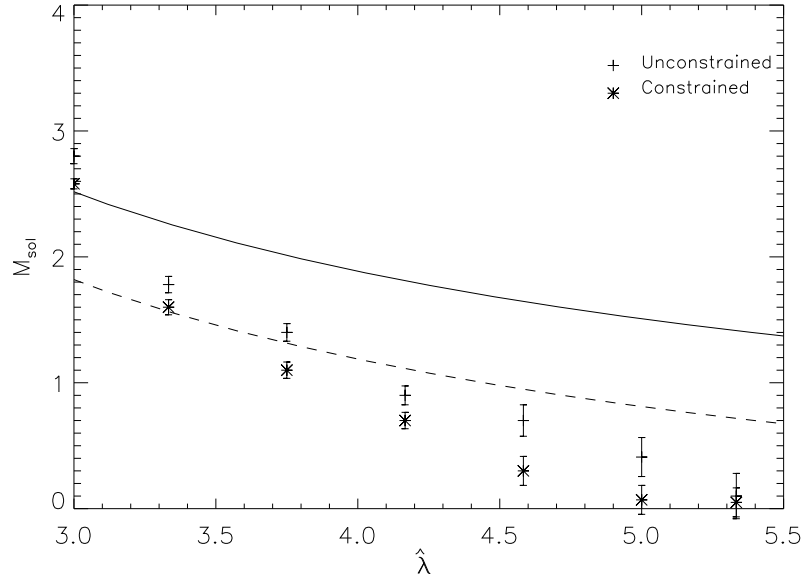


FIG. 6. Plot of soliton mass versus β with $\hat{m}^2 = -4$. The Monte Carlo results are compared with the classical (solid line) and semiclassical results (dashed line).